

Metastability And Plasticity In A Conceptual Model of Neurons

Bo Deng¹

Abstract: For a new class of neuron models we demonstrate here that typical membrane action potentials and spike-bursts are only transient states but appear to be asymptotically stable; and yet such metastable states are plastic — being able to dynamically change from one action potential to another with different pulse frequencies and from one spike-burst to another with different spike-per-burst numbers. The pulse and spike-burst frequencies change with individual ions' pump currents while their corresponding metastable-plastic states maintain the same transmembrane voltage and current profiles in range. It is also demonstrated that the plasticity requires two one-way ion pumps operating in opposite transmembrane directions to materialize, and if only one ion pump is left to operate, the plastic states will be lost to a rigid asymptotically stable state either as a resting potential, or a limit cycle with a fixed pulse frequency, or a spike-burst with a fixed spike-per-burst number. These metastable-plastic pulses and spike-bursts may be used as information-bearing alphabet for a communication system that neurons are thought to be.

1. Introduction. A neuron is an information processing unit either as a signal transmitter or a signal receiver or both. A communication system must have an alphabet to code information and each symbol of the alphabet must be represented by a physical state of the system. A communication system is also a dynamical process in which information is coded and decoded in real time. Thus, an efficient communication system should process the physical alphabet states in transient, not to wait for the system to settle down to its asymptotic states. A reliable communication system, on the other hand, should have the transient alphabet states to behave like steady states, having robust and distinct profiles for high tolerance to small deterministic perturbations as well as nondeterministic noises. That is, an efficient and reliable communication system needs to have both ways for its alphabet handling. In addition, a functional communication system must be able to shift from one alphabet state to another for information encoding and decoding. A transient state behaving like a steady state is referred to as *metastable*. The capability to internally shift from one metastable alphabet state to another is referred to as *plastic*.

The purpose of this paper is to demonstrate that for a class of neuron models introduced in [4] they do possess both properties of metastability and plasticity, and that both properties are mediated by two ion pumps. More specifically, the neuron models treat the passive electromagnetic current and the passive diffusive current of an ion species differently from the ion's active current through a one-way ion pump, with the passive currents modeled by nonlinear resistors and the ion pumps

¹Department of Mathematics, University of Nebraska-Lincoln, Lincoln, NE 68588. Email: bdeng1@math.unl.edu

modeled by one-way inductors. It was shown in [4] that under the key assumption of having only one one-way ion pump (with current A_1), among some other reasonable conditions, action potentials (pulses) and spike-bursts can be generated, which are referred to as the *native action potentials* and the *native spike-bursts*, respectively. In this paper, we will show that if a second, opposite-directional ion pump is included (with current $-A_2$), then all the sudden a new, parallel dimension is added to the phase space where the native pulses and spike-bursts reside, and the native pulses and spike-bursts can then roam into the new dimension and change their temporal profile from one frequency or spike-per-burst number to another frequency or another spike-per-burst number, but all the while maintaining their transmembrane voltage and current profiles from their native phase space for many temporal episodes as if they were asymptotically stable. The new dimension that allows the metastable-plastic pulses and spike-bursts to exist is defined precisely by the absolute sum of the ion pump currents, $I_S = |A_1| + |A_2|$, which will collapse onto the net transmembrane-pump-current dimension $I_A = A_1 - A_2$ when the second pump is shut and closed ($A_2 \equiv 0$), which in turn will collapse the new plasticity dimension onto the native phase space itself, wiping out all the meta expatriates.

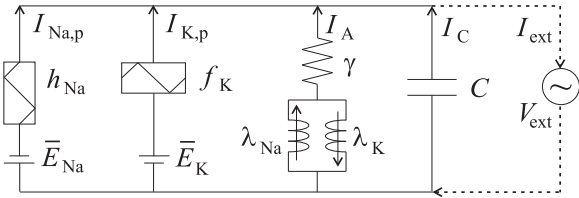
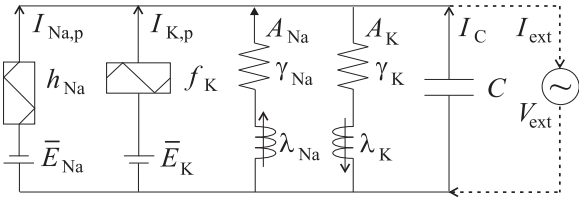
Since ion pumps require neuron cell's ATP-to-ADP biochemical energy conversion to operate, these results suggest a possible direct link between cellular metabolism and possible electrophysiological mechanism for neural metastability and plasticity. These results also support the view that the membrane action potentials and spike-bursts can be viewed as alphabet states ([7, 13]) for a communication system that neurons are thought to be.

2. The Mathematical Models. We will describe the neuron models here with sufficiently self-contained essentials to construct them. We refer to [4] for a more comprehensive review.

First, the conceptual model of a neuron is conventional: the bilipid cell membrane is modeled as a capacitor, and there are various transmembrane channels for ion transportation which can be thought all in parallel at this point until an exception is to be made otherwise later. There are two types of ion current channels: the passive channels and the active channels. And the passive channels are further divided into two kinds: the electro channel due to the electromagnetic force of all ions, and the diffusive channel for a particular ion species due to that ion species's transmembrane concentration. The active channels are made of ion pumps which transport individual ion species in a fixed transmembrane direction: either inward or outward. The passive channels are not related to biochemical energy conversion but the ion pumps are.

Here comes one of the key differences between our models and others in how to model these channels. For our models, the electro channels are modeled by conductors (resistors) whose IV -characteristic is monotonically increasing with $g \geq 0$ denoting the maximal slope which is the conductance (usually considered in a relevant range of the voltage and current). The diffusive channels are modeled by diffusors (negative resistors) because its effect is exactly opposite to the electromagnetic force. As a result, the diffusive channel's IV -characteristic is monotonically decreasing with $d \leq 0$ denoting the minimal (or maximal in magnitude) slope which is referred to as the diffusion coefficient. The conductors are used to model directly the current-voltage relation-

Table 1: Model Taxon, Circuit Diagram, and Equivalent Equations

| The pK^+sNa^+ Model | The $\text{pK}^+_{-d}\text{sNa}^+_{+d}$ Model |
|---|--|
|  $\begin{cases} CV_C' = -[I_{\text{Na,p}} + f_K(V_C - \bar{E}_K) \\ \quad + A_{\text{Na}} - A_K - I_{\text{ext}}] \\ A_{\text{Na}}' = \lambda_{\text{Na}} A_{\text{Na}} [V_C - \gamma(A_{\text{Na}} - A_K)] \\ A_K' = \lambda_K A_K [-V_C + \gamma(A_{\text{Na}} - A_K)] \\ \epsilon I_{\text{Na,p}}' = V_C - \bar{E}_{\text{Na}} - h_{\text{Na}}(I_{\text{Na,p}}). \end{cases}$ |  $\begin{cases} CV_C' = -[I_{\text{Na,p}} + f_K(V_C - \bar{E}_K) \\ \quad + A_{\text{Na}} - A_K - I_{\text{ext}}] \\ A_{\text{Na}}' = \lambda_{\text{Na}} A_{\text{Na}} [V_C - \gamma_{\text{Na}} A_{\text{Na}}] \\ A_K' = -\lambda_K A_K [V_C + \gamma_K A_K] \\ \epsilon I_{\text{Na,p}}' = V_C - \bar{E}_{\text{Na}} - h_{\text{Na}}(I_{\text{Na,p}}). \end{cases}$ |

ship of ions' electromagnetic gating mechanism while the diffusors are used to do the same but for ions' diffusive gating mechanism instead. Such gating mechanisms are modeled differently by Hodgkin-Huxley type models which treat them in terms of gating probability evolution. In this regards, our approach seems more phenomenological but with a trade-off gain in simplicity, and more importantly in practicality because resistors and negative resistors are ubiquitous components in circuitry.

After the resistor/negative-resistor assumptions on the passive electro and diffusive channels comes the question of connectivity. The connectivity of a particular ion's passive channels can be one of two configurations: the electro and the diffusive currents going through separate parallel channels; the electro and the diffusive currents going through a same channel. The former is referred to as a *parallel conductor-diffusor* and the latter is referred to as a *serial conductor-diffusor*. Each configuration will give rise to a distinct characteristic to its joint IV -curve by Kirchhoff's Current and Voltage Laws. For the parallel connectivity, the total current of that ion species is always a function of the common voltage over the parallel, $I = f(V)$. For the serial connectivity, the total voltage across the series is always a function of the common current through the series, $V = h(I)$. When becoming truly nonlinear, the parallel IV -characteristic, $I = f(V)$, usually takes the shape of the letter “ N ”, whereas the serial IV -characteristic, $V = h(I)$, usually takes the shape of the letter “ S ”.

For a parallel conductor-diffusor, let $g \geq 0$ be the maximal conductance of the conductor and $d \leq 0$ be the minimal diffusion constant of the diffusor. Then the parallel conductor-diffusor has an S -characteristic if $g + d < 0$ and the IV -curve $I = f(V)$ is decreasing in a finite voltage interval $[v_1, v_2]$. Similarly, the serial conductor-diffusor has an N -characteristic if $1/g + 1/d < 0$

or $g + d > 0$, and the IV -curve $V = h(I)$ is decreasing in a finite interval $[i_1, i_2]$. As demonstrated in [4], the generation of action potentials require the parallel N -nonlinearity of an ion species, and the generation of spike-bursts requires the parallel N -nonlinearity of one ion species and the serial S -nonlinearity of another ion species. When a conductor-diffusor is decomposed into the sum of a linear resistor and a ramp-like diffusor, the form is called canonical. One justification for the canonical decomposition is the reason that the electromagnetic force affects all ion species in all the voltage range, whereas the diffusive force of a particular ion only affects that ion's transmembrane flux in a finite range, outside of which the ion's concentration on a given side of the cell will saturate in one extreme or another, giving rise to a ramp-like characteristic.

The active channel of a given ion species consists of an ion pump for the ion species. An ion pump is assumed to be fundamentally different from the passive channels in a couple ways. First, ions are assumed to spiral their way through a pump rather in a straight manner. Second, a particular ion species is transported only in a fixed directionality: either into the cell or outside but not both, e.g., Na^+ is pumped out from the cell and K^+ is pumped into the cell. The first assumption makes an ion pump to behave like an inductor, and the second property makes it to be a one-way inductor. As a result, a particular ion species's pump current, A , and the voltage across the pump, V , are modeled by the relation, $A' = \lambda AV$, where $\lambda > 0$ is called the ion's pump coefficient. It is the IV -characteristic of a variable inductor whose inductance is mediated by its current to fix the directionality of the pump: $A(t) > 0$ if and only if $A(0) > 0$. One important consequence ([4]) of these assumptions of ion pumps is that the directionality of an ion pump implies the polarity of that ion's active and passive resting potentials: an outward (resp. inward) cation pump resulting in a positive (resp. negative) extracellular resting potential of the cation.

As shown in [4], these assumptions about a neuron can be systematically captured by a model taxonomy, or a circuit diagram, or a system of differential equations, each is qualitatively equivalent to another in model description. Table 1 gives an illustration for this methodology, showing what is called a pK^+sNa^+ model and a $\text{pK}^+_{-d}\text{sNa}^+_{+d}$ model, using K^+ and Na^+ as prototypical ion species for illustration. Of the model notation, “ pK^+ ” stands for K^+ 's passive channels in *parallel* connectivity while “ sNa^+ ” stands for Na^+ 's passive channels in *serial* connectivity. If the parallel (resp. serial) connection does not produce a true nonlinearity in the shape of N (resp. S), the model is denoted by as cK^+sNa^+ (resp. pK^+cNa^+) with “ c ” standing for conductor domination over its diffusor counterpart. Because the conductive channel is always a part of a conductor-diffusor combination, a cX model can always be considered as a subsystem of a pX and an sX model, and, similarly, a cXyY model is a subsystem of a pXyY model and an sXyY model.

The \pm signs for the subscript, on the other hand, denote the ion pumps' directionality with K^+ pumped into the cell ($-$) and Na^+ pumped out the cell ($+$). Without a designation d , the pumps are assumed to share a common parallel structure which in turn has a parasitic resistance γ . With it, the pumps are assumed to operate independently on their own with distinct pump coefficients and distinct parasitic pump resistances. A subscript “ 0 ”, on the other hand, means the absence of an ion pump for the referred ion species, as for the class of $\text{pK}^+\text{sNa}^+\text{cCl}_0^-$ models.

Similarly description applies to other types of models, e.g., pNa^+sK^+ models are the same as pK^+sNa^+ models except that Na^+ 's passive channels are in parallel and K^+ 's passive channels are in series with the polarities of the passive resting potentials and the directionalities of the ion pumps remain unchanged.

For circuit diagrams from Table 1, a vertical box circumscribing a letter S stands for the serial connectivity of the electro and diffusive currents of an ion species and a horizontal box circumscribing a letter N stands for the parallel connectivity of the electro and diffusive currents of an ion species. So a horizontal N -box always goes with the pX taxon and a vertical S -box with the sY taxon. As mentioned earlier, the S -nonlinearity and the N -nonlinearity are the most typical nonlinearities a serial conductor-diffusor and a parallel conductor-diffusor will have, respectively.

The default current direction is chosen to be from the inside of cell to the outside, with the exception given to the external forcing current I_{ext} , and the ion pump directions which are fixed: $A_{\text{Na}} > 0$ is always outward and $-A_{\text{K}} < 0$ is always inward. However, the net Na^+ - K^+ ion pump current is $I_{\text{A}} = A_{\text{Na}} - A_{\text{K}}$ with the outward direction set as its default. Thus, the directed inductor symbols stand for ion pumps which can be combined in a sub-parallel group when the pump structure is a shared parallel or be separated in a disjoint parallel. As mentioned above, we will assume that the polarity of an ion's passive resting potential is automatically fixed by its pump directionality, as in the cases of $\bar{E}_{\text{K}} < 0$ and $\bar{E}_{\text{Na}} > 0$, respectively. The corresponding models with $\bar{E}_{\text{K}} > 0$ or $\bar{E}_{\text{Na}} < 0$ cannot generate any oscillation as if for dead cells, nor be consistent with an empirical fact that the active resting potentials for K^+ and Na^+ are negative and positive, respectively. Thus, the circuit diagram and its model taxon uniquely define each other leaving only the particular functional forms for the parallel and serial IV -characteristics to be specified.

For pK^+sNa^+ model's system of differential equations from Table 1, $I = f_{\text{K}}(V)$ defines the parallel IV -characteristic of K^+ 's passive channels, which is always a function of V by Kirchhoff's Current Law. Also, $V = h_{\text{Na}}(I)$ defines the serial IV -characteristic of Na^+ 's passive channels, which is always a function of I by Kirchhoff's Voltage Law. The first equation of the circuit system is derived from Kirchhoff's Current Law that the sum of all transmembrane currents is conserved at 0 and the device characteristic for the bilipid membrane as a linear capacitor: $CV'_C = I_C$. The second and third equations are for the ion pumps, and, depending on whether or not the pumps are joint or disjoint, they are slightly different as shown. The last equation is a standard practical approximation ([2]) for the serial conductor-diffusor's IV -characteristics. More specifically, for sufficiently small $\epsilon > 0$, the equation quickly equilibriumizes to the $I_{\text{Na,p}}$ -nullcline which is purposely set to be the IV -curve of Na^+ 's serial conductor-diffusor. This is especially necessary when the serial IV -curve shapes like an S , a so-called S -hysteresis for which the current cannot be explicitly solved in terms of the voltage. Note also that the circuit diagrams and the circuit equations from Table 1 uniquely define each other as well.

Similarly, for a pNa^+sK^+ model, $I = f_{\text{Na}}(V)$ defines the parallel IV -characteristic of Na^+ 's passive channels and, respectively, $V = h_{\text{K}}(I)$ defines the serial IV -characteristic of K^+ 's passive channels, and both are left to be specified.

Table 2: *IV*-Characteristic Curves

| | <i>S</i> -Nonlinearity | <i>N</i> -Nonlinearity |
|--------------------------------|---|---|
| | $V = h_{\text{Na}}(I)$ | $I = f_{\text{K}}(V)$ |
| $\text{pK}_*^+ \text{sNa}_*^+$ | <ul style="list-style-type: none"> • piecewise linear curve: $V = \frac{1}{g_{\text{Na}}}I + \frac{1}{d_{\text{Na}}}(I - i_1)(i_1 < I < i_2) + \frac{1}{d_{\text{Na}}}(i_2 - i_1)(i_2 < I)$ • smooth curve: $V = -\frac{\frac{2}{g_{\text{Na}}} + \frac{2}{d_{\text{Na}}}}{(i_2 - i_1)^2}[(I - i_1)(I - i_2)^2 - \frac{1}{3}(I - i_2)^3 + i_1 i_2^2 - \frac{1}{3}i_2^3]$ | $I = g_{\text{K}}V + d_{\text{K}}(V - v_1)(v_1 < V < v_2) + d_{\text{K}}(v_2 - v_1)(v_2 < V)$ $I = -\frac{2(g_{\text{K}} + d_{\text{K}})}{(v_2 - v_1)^2}[(V - v_1)(V - v_2)^2 - \frac{1}{3}(V - v_2)^3 + v_1 v_2^2 - \frac{1}{3}v_2^3]$ |
| | $V = h_{\text{K}}(I)$ | $I = f_{\text{Na}}(V)$ |
| $\text{pNa}_*^+ \text{sK}_*^+$ | <ul style="list-style-type: none"> • piecewise linear curve: $V = \frac{1}{g_{\text{K}}}I + \frac{1}{d_{\text{K}}}(I - i_1)(i_1 < I < i_2) + \frac{1}{d_{\text{K}}}(i_2 - i_1)(i_2 < I)$ | $I = g_{\text{Na}}V + d_{\text{Na}}(v_1 - v_2)(V < v_1) + d_{\text{Na}}(V - v_2)(v_1 < V < v_2)$ |
| | Conditions: $g_{\text{J}} > 0, d_{\text{J}} < 0, g_{\text{J}} + d_{\text{J}} > 0$ with $\text{J} = \text{Na}^+, \text{ or } \text{K}^+$ | Conditions: $g_{\text{J}} > 0, d_{\text{J}} < 0, g_{\text{J}} + d_{\text{J}} < 0$ with $\text{J} = \text{Na}^+, \text{ or } \text{K}^+$ |

To complete any model for simulation, Table 2 gives some specific *IV*-characteristic functional forms for both ions. Here, the voltage range $[v_1 + \bar{E}_{\text{J}}, v_2 + \bar{E}_{\text{J}}]$ is dominated by ion J's transmembrane diffusion over its parallel electro channel, and the same for the current range $[i_1, i_2]$ for another ion's diffusive channel over its serial electro channel instead. The list includes one type of piecewise linear functionals, which are canonical. More specifically, using the *N*-characteristic, $I = f_{\text{K}}(V)$, as an example, $I = g_{\text{K}}V$ represents the canonical conductor, and $I = d_{\text{K}}(V - v_1)(v_1 < V < v_2) + d_{\text{K}}(v_2 - v_1)(v_2 < V)$ represents the ramp-like canonical diffuser. Notation $(a < x < b)$ with $a \geq -\infty, b \leq +\infty$ is a `Matlab` convention for step functions: $(a < x < b) = 1$ if $a < x < b$ and $(a < x < b) = 0$ otherwise. With $a = -\infty$ or $b = +\infty$, the notation is simplified to be $(a < x < b) = (x < b)$ or $(a < x < b) = (a < x)$, respectively. The list includes one type of smooth functions which is quite different from the listed piecewise-linear type in shape. Another smooth and canonical type is given in [4] which, on the other hand, is very close in shape to the piecewise-linear type. The dissimilarity of the cubic type from the piecewise-linear type is used to demonstrate the metastable-plastic phenomenon for a wider range of functional forms. A general method to generate all such functionals is also given in [4].

3. The Result. For more direct insights into some of the circuit models, it is more convenient

Table 3: Circuit Equations in $V_C I_A I_S I_{J,p}$ Variables

| The $\text{pK}^+_{-}\text{sNa}^+_{+}$ Model | The $\text{pNa}^+_{+}\text{sK}^+_{-}$ Model |
|---|---|
| $\begin{cases} CV'_C = -[I_{\text{Na},p} + f_K(V_C - \bar{E}_K) \\ \quad + I_A - I_{\text{ext}}] \\ I'_A = \lambda I_S[V_C - \gamma I_A] \\ I'_S = \lambda I_A[V_C - \gamma I_A] \\ \epsilon I'_{\text{Na},p} = V_C - \bar{E}_{\text{Na}} - h_{\text{Na}}(I_{\text{Na},p}) \end{cases}$ | $\begin{cases} CV'_C = -[I_{K,p} + f_{\text{Na}}(V_C - \bar{E}_{\text{Na}}) \\ \quad + I_A - I_{\text{ext}}] \\ I'_A = \lambda I_S[V_C - \gamma I_A] \\ I'_S = \lambda I_A[V_C - \gamma I_A] \\ \epsilon I'_{K,p} = V_C - \bar{E}_K - h_K(I_{K,p}) \end{cases}$ |

to cast their circuit equations in another equivalent form by a change of variables for the pump currents A_{Na}, A_K as bellow,

$$\begin{cases} I_A = A_{\text{Na}} - A_K \\ I_S = A_{\text{Na}} + A_K \end{cases} \quad \text{equivalently} \quad \begin{cases} A_{\text{Na}} = \frac{1}{2}(I_S + I_A) \\ A_K = \frac{1}{2}(I_S - I_A) \end{cases}$$

Here, I_A is the net current for the $\text{Na}^+ \text{-K}^+$ ion pump whereas I_S is the absolute sum of the individual pump currents, which is expected to correlate with the ATP-to-ADP energy conversion of the neuron cells. It is straightforward to check that the equivalent systems for the $\text{pK}^+_{-}\text{sNa}^+_{+}$ model and the $\text{pNa}^+_{+}\text{sK}^+_{-}$ model are as listed in Table 3. The equations in I_A and I_S for the $\text{xK}^+_{-}\text{yNa}^+_{+d}$ models are not as clean nor convenient as for the $\text{xK}^+_{-}\text{yNa}^+_{+}$ counterparts, and they are not shown here. As it will become clear later that the advantage to use the $I_A I_S$ -form of the equations for the $\text{xK}^+_{-}\text{yNa}^+_{+}$ models is the fact that the total absolute pump current I_S -variable is decoupled from the rest of the equations, and the fact that I_S 's nontrivial nullcline, $V_C = \gamma I_A$, coincides that of I_A 's nullcline.

For the discussion on ion pump currents earlier in the Introduction, we have correspondingly $A_1 = -A_K$ and $A_2 = -A_{\text{Na}}$. Thus, without the Na^+ pump $A_{\text{Na}} \equiv 0$, the native K^+ phase space $V_C A_K I_{\text{Na},p}$ corresponds to the 3-dimensional subspace $I_A = -I_S$ of the full 4-dimensional $V_C I_A I_S I_{\text{Na},p}$ -space. It is useful to notice that for the $\text{pK}^+_{-}\text{sNa}^+_{+}$ (resp. $\text{pNa}^+_{+}\text{sK}^+_{-}$) models, whatever the nulleline configurations the $V_C, I_A, I_{\text{Na},p}$ (resp. $I_{K,p}$) equations define in the native subspace $I_A = -I_S$, they will automatically extend without alteration into the full space parallelly along the I_S -axis.

Regarding the metastability and plasticity of action potentials and spike-bursts, some relevant results of [4] are summarized here. It was demonstrated that to depolarized the membrane from its resting potential, ion diffusion against concentration gradient across the cell membrane must dominate in some membrane potential range (i.e. $[v_1 + \bar{E}_J, v_2 + \bar{E}_J]$). More specifically, action potentials require only one ion species's diffusion domination over its conductive channel in parallel. They are the prominent feature of pXcY or just simply pX models. On the other hand, spike-bursts require one ion species' diffusion domination over its conductive channel in parallel

for the burst and another ion species' diffusion domination over its conductive channel in series for the spikes (i.e. over a current range $[i_1, i_2]$). They are the prominent feature of pXsY models. Thus, K^+ -mediated action potentials are the result of K^+ 's parallel diffusion domination in pK_{\pm}^+ and $pK_{\pm}^+sNa_{\pm}^+$ models. Similarly, Na^+ - K^+ spike-bursts are the result of K^+ 's parallel diffusion domination for the burst and Na^+ 's serial diffusion domination for the spikes in $pK_{\pm}^+sNa_{\pm}^+$ models. Likewise, Na^+ -mediated action potentials and K^+ - Na^+ spike-bursts are among the prominent dynamical features of $pNa_{\pm}^+sK_{\pm}^+$ models. Furthermore, the presence of an ion pump for the ion species having passive channels in parallel is absolutely essential for action potential generation as well as for spike-burst generation — shutting it down turns off both types of spiking activities. For examples, $pK_{\pm}^+sNa_0^+$ type models permit both types of spiking activities, referred to as *native action potentials* and *native spike-bursts*, respectively, but $pK_0^+sNa_{\pm}^+$ do not. In other words, there are native oscillatory inhabitants in the $V_C A_K I_{Na,p}$ -space but not in the $V_C A_{Na} I_{Na,p}$ -space, and the roaming metastable-plastic oscillations into the full space $V_C A_K A_{Na} I_{Na,p}$ -space (or equivalently the $V_C I_A I_S I_{Na,p}$ -space) are the result of the addition of the Na^+ pump, opposite in directionality against the K^+ pump.

3.1. Action Potential Metastability and Plasticity for pXyY Models. As demonstrated in [4], the K^+ -mediated (resp. Na^+ -mediated) action potentials are among the prominent features of pK_{\pm}^+ type (resp. pNa_{\pm}^+ type) models for which the effective region of the action potentials is not affected by the diffusion domination of ion Na^+ (resp. K^+). Certain but typical conditions need to be satisfied for their generation. Chief among them is the condition of K^+ 's (resp. Na^+ 's) diffusion domination of all passive conductive channels. For the $pK_{\pm}^+sNa_{\pm}^+$ (resp. $pK_{\pm}^+sNa_{\pm}^+$) models, the condition is.

$$d_K + g_K + g_{Na} < 0 \quad (\text{resp. } d_{Na} + g_{Na} + g_K < 0).$$

As an example, Fig.1 shows that if action potentials are permitted in a $pK_{\pm}^+sNa_{\pm}^+$ model, they must be metastable and plastic transient states.

The simulations are for the $pK_{\pm}^+sNa_{\pm}^+$ circuit equations with the piecewise linear functionals f_K, h_{Na} from Table 2. Here, the K^+ -mediated action potentials are also referred to as K^+ -pulses, or just pulses for short. The start of a pulse is defined when the membrane potential V_C crosses the I_A -nullcline surface (which coincides I_S 's nontrivial nullcline surface) while increasing. A pulse terminates when the membrane voltage crosses the same surface but while decreasing. The pulse period (resp. frequency) is the time (resp. the reciprocal of) between the start and the end of a pulse. The pulse refractory period is the time between the end of a pulse and the start of the next pulse.

At a first glance, Fig.1(a) appears to show five distinct limit cycles. But, in fact, the only limit cycle is the dashed cycle which is the native cycle on the native subspace $I_A = -I_S$ when the Na^+ pump is shut off ($A_{Na}(0) = 0$). In this case, Na^+ 's transmembrane diffusion does not dominate in the effective region of the action potentials, and as a result, the $I_{Na,p}$ -equation can be solved exactly with $\epsilon = 0$ and $I_{Na,p} = g_{Na}(V_C - \bar{E}_{Na})$ in the effective region. Substituting this relation into the first V_C -equation and eliminating the A_{Na} -equation since $A_{Na}(0) = 0$ from the $pK_{\pm}^+sNa_{\pm}^+$ equations of

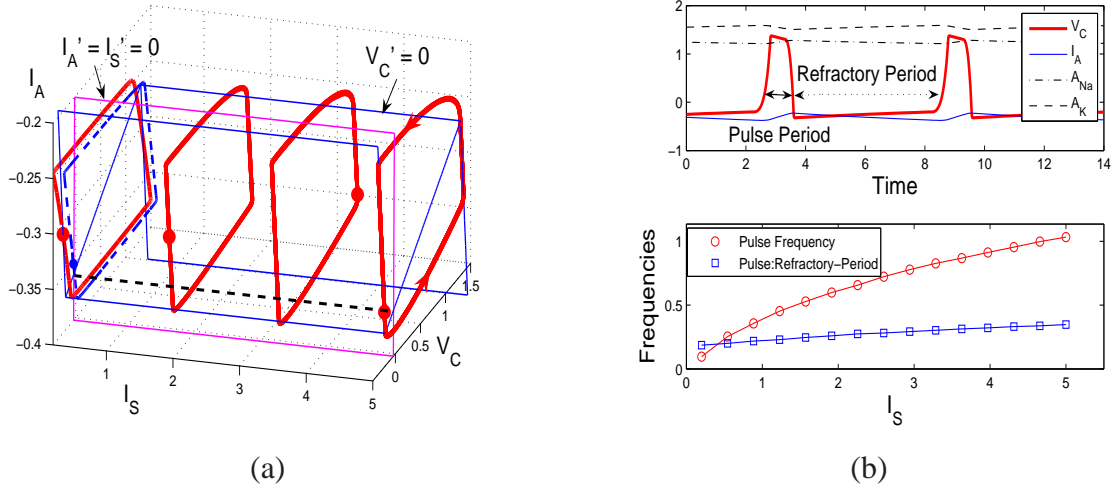


Figure 1: Dimensionless simulations of a pK^+sNa^+ model with parameter values: $g_{\text{Na}} = 0.17$, $d_{\text{Na}} = -0.06$, $i_1 = 0.5$, $i_2 = 1$, $\bar{E}_{\text{Na}} = 0.6$, $g_{\text{K}} = 1$, $d_{\text{K}} = -1.25$, $v_1 = 0.5$, $v_2 = 2$, $\bar{E}_{\text{K}} = -0.7$, $C = 0.01$, $\lambda = 0.05$, $\gamma = 0.1$, $I_{\text{ext}} = 0$, $\epsilon = 0.001$. (a) The phase portrait in the $I_S V_C I_A$ -space with the native limit cycle (dashed cycle) and 4 transient orbits (solid cycles). The 2-dimensional nullcline configuration for the V_C, I_A variables extends cylindrically into the I_S -dimension. (b) Top panel, time series plot for a typical pulse train. Bottom panel, showing the frequency of K^+ -pulses, and the ratio of the pulse period over the refractory period between adjacent pulses, all averaged over integration time interval $[0, 50]$ for each selected I_S value.

Table 1 lead to a 2-dimensional system. As a result, the native attractor is a limit cycle. However, when the Na^+ pump is on with $A_{\text{Na}}(0) > 0$, the A_{Na} -equation is included in the system which now becomes 3-dimensional. The four solid pieces of Fig.1(a) are only transient orbits over different ranges of the absolute pump current variable I_S . (This point becomes obvious in the simulation Fig.3(e,f) for a $\text{pK}_{-d}^+\text{sNa}_{+d}^+$ model.) Notice that every pulsing episode in the $V_C I_A$ -profile tracks around the same V_C -nullcline surface, appearing asymptotically stable, but nonetheless drifting slowly in the absolute pump current I_S .

The top panel of Fig.1(b) shows a typical train of pulses in time-series. The bottom panel of Fig.1(b) shows the averaged pulse frequency over a fixed time period $t = 50$ for a discrete set of starting I_S value. Notice from the frequency plot that the greater I_S , the greater the spike frequency. This is perfectly consistent with the I_A equation for which $I_S(t)$ can be viewed as a positive proportionality coefficient for the rate of change $I_A'(t)$, and the greater the I_S , the shorter the period of the metastable pulse. Also notice that the ratio of the spike period over its refractory period changes little.

3.2. Spike-Burst Metastability and Plasticity for pK^+sNa^+ Models. Similarly, the Y-spike-X-bursts are among the primary features of pXsY models for which the effective region is affected by the diffusion domination of both ion species. Again, certain but typical conditions need to be

satisfied for their generation. Chief among them for a pK^+sNa^+ model is the same K^+ 's diffusion domination condition

$$d_K + g_K + g_{\text{Na}} < 0$$

and the condition of Na^+ 's diffusion intervention

$$h_{\text{Na}}(i_1) + \bar{E}_{\text{Na}} < v_2 + \bar{E}_K.$$

Fig.2 shows that if Na^+ -spike- K^+ -bursts exist in a pK^+sNa^+ model, they must be metastable and plastic transient states.

Here, the generation of spike-bursts can be described briefly as follows. What is an X-mediated action potential for a pX type model now becomes an X-mediated burst for a corresponding pXsY type model. More specific, the start and the end of a burst for the pXsY model take place at the same locations on the $I_A I_S$ -nullcline surface as the action potentials do for the pX model. But unlike the action potentials, now Y's diffusion does intervene, and the interrupted action potential is now referred as a *burst*. In addition, the Y-mediated spikes are then inserted into the intervened period of the burst. For the simulation, the start and the end of a Y-spike are defined when the corresponding orbit crosses the middle voltage value, $\bar{E}_Y + [h_Y(i_1) + h_Y(i_2)]/2$, of the S-shape characteristic of ion Y's serial conductor-diffusor when the membrane voltage increases and decreases, respectively. The spike period and frequency are defined similarly.

Fig.2(a) shows the time-series of a typical spike-burst. The isospike number 3 would remain fixed for many more bursts before changing to 2 or 4 depending on specific models. That is, they appear to be asymptotically stable over a finite and long period of time, but are not in actuality. Fig.2(b) shows the native spike-burst in dots and a few metastable spike-bursts in solid with isospike number equal to 7, 3, 2, 1, respectively, each restarted at a different value of I_S . If one starts at the left most 7-isospike burst and continues the simulation for the entirely transition to reach the 1-isospike burst, the plot would show all the isospiking bursts, and all the n -to- $(n-1)$ bursting transitions. Various measurements of the isospike bursts are collected in Fig.2(c). It includes the spike frequency — the reciprocal of the averaged time between the start and the end of a spike during a burst; the burst frequency which is similarly defined; the refractory-period which is the time from the end of a burst to the start of the next burst. The figure also shows the ratio of the burst-period to the refractory-period as a function of the absolute current. It also shows the isospike number plot. Notice that the spike frequency (SF), the burst frequency (BF), and the isospike number (IN) are related by $\text{SF} = \text{BF} \times \text{IN}$.

Fig.2(d) shows a rough partial partition for isospike bursts in terms of individual ion pump currents. It is the same partition in the I_A, I_S variables but translated to the A_{Na}, A_K variables. The region below the dash line corresponds to $I_A = A_{\text{Na}} - A_K > I_A^*$ (whose definition is defined below). This region is then partitioned by lines $I_S = A_{\text{Na}} + A_K = \text{constant}$, which in reality should be interpreted as a narrow region in which transitions of n -to- $(n-1)$ isospike bursts take place. The planar region should be interpreted as an open region in the full state space with the $V_C, I_{\text{Na,p}}$ variables hidden from the view. In fact, the full open region contains the joint, attractive (or

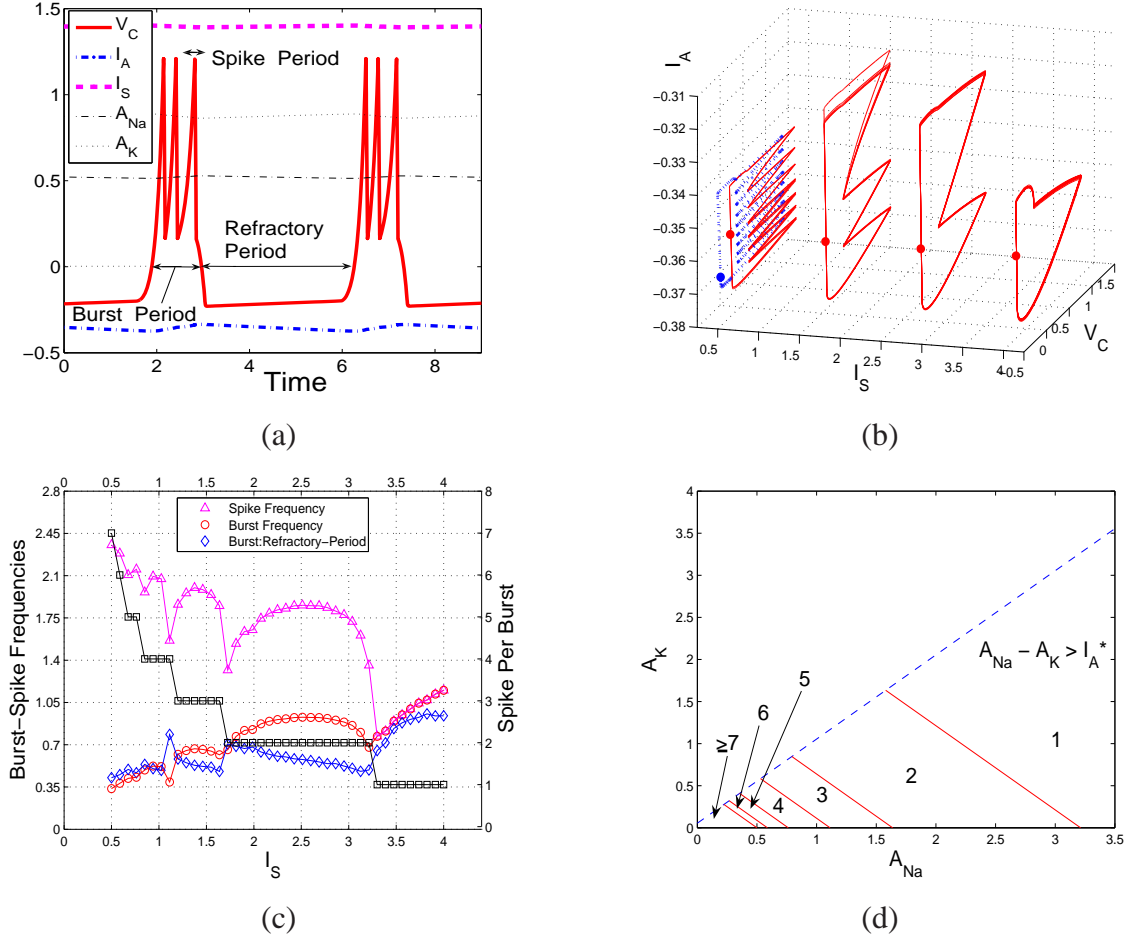


Figure 2: (a) The time-series plot for a typical spike-burst. (b) The dotted spike-burst is the native spike-burst in the invariance space $I_A = I_S$ (or $A_{Na} = 0$). Metastable 7-, 3-, 2-, 1-isospike bursts are shown along the I_S -axis. (c) Various frequencies plot. (d) A rough partition of metastable isospiking bursts in terms of individual ion pump currents, with other variables occupying an open region around the attracting branch of the $V_C I_{Na,p}$ -nullcline corresponding to the refractory phase of the spike-bursts.

conductive) branch of the $V_C I_{\text{Na,p}}$ -nullcline on $I_{\text{Na,p}}$'s nullcline surface, which in turn corresponds to the refractory phase of the spike-bursts (see [4] for a more detailed geometric illustration on the nullcline surfaces). Here, the joint conductive branch ends when K^+ 's diffusion becomes dominant. In the voltage range for the piecewise-line case, K^+ 's diffusive domination occurs in $[v_1 + \bar{E}_K, v_2 + \bar{E}_K]$. Corresponding to the left critical value $v_1 + \bar{E}_K$, K^+ 's diffusive domination starts at the I_A^* value in the I_A variable. For any initial point from the n -isospike region, the immediate transient burst has exactly n spikes. The start of all bursts takes place precisely at the I_A^* value in the I_A variable and at $v_1 + \bar{E}_K$ in the V_C variable, respectively.

3.3. Spike-Burst Metastability and Plasticity of Other Models. To show the ubiquity of metastable-plastic spike-bursts, three different models are used here. We begin with an alternative $\text{pK}^+ \text{sNa}^+$ model from Table 1 for which the cubic polynomial functions from Table 2 are used for K^+ 's N -shaped characteristic and Na^+ 's S -shape characteristic. The functional forms are significantly different from the piecewise-linear ones, preserving only the properties that $[v_1, v_2]$ and $[i_1, i_2]$ are the diffusion dominated ranges for K^+ , Na^+ , respectively. By the method of [4], all the functional forms can be determined from their derivatives in general, and for the cubic polynomials in particular, they are obtained as below:

$$f_K'(V) = -\frac{4(g_K + d_K)}{(v_2 - v_1)^2}(V - v_1)(V - v_2), \text{ and } f_K(V) = \int_0^V f_K'(v)dv,$$

$$h_{\text{Na}}'(I) = -\frac{\frac{4}{g_{\text{Na}}} + \frac{4}{d_{\text{Na}}}}{(i_2 - i_1)^2}(I - i_1)(I - i_2), \text{ and } h_{\text{Na}}(I) = \int_0^I h_{\text{Na}}'(i)di.$$

A simulation is shown in Fig.3(a,b). Fig.3(c,d) shows a simulation of the $\text{pNa}^+ \text{sK}^+$ equations from Table 3 with the piecewise-linear IV -curves from Table 2. And last, Fig.3(e,f) shows a simulation of the $\text{pK}^+ \text{sNa}^+$ equations from Table 1 with the piecewise-linear IV -curves from Table 2. Unlike the others, the absolute pump current I_S drifts down and at a faster rate. This is true for both the spike-bursts as shown and the action potentials not shown. Again, dotted curves are for the native spike-burst attractors.

3.4. Spike Atrophy — Loss of Plasticity with One Ion Pump. As mentioned earlier that the native action potential is a 2-dimensional limit cycle on a planar subspace of the invariant space $I_A = -I_S$ when the Na^+ pump is shut ($A_{\text{Na}} = 0$). We can see from Fig.1(a) that the metastable-plastic pulses exist only in the extended space along the I_S -axis when the second pump is turned on. We can also see that when projected onto the subspace $I_A = -I_S$ along the I_S -axis, all the meta pulses take up the same profile as the native limit cycle because the nullcline configuration of the equations that determines the shape of the oscillations is independent of the I_S variable. Because the system is autonomous and the metastable-plastic pulses occupy the same $V_C I_A$ -phasespace under projection, they cannot exist without the extra dimension provided by I_S , or equivalently the second opposite-directional Na^+ pump.

The same argument and conclusion can also be made for spike-bursts. In particular, without the Na^+ pump, the system is 3-dimensional and the spike-burst is a 3-dimensional structure. The

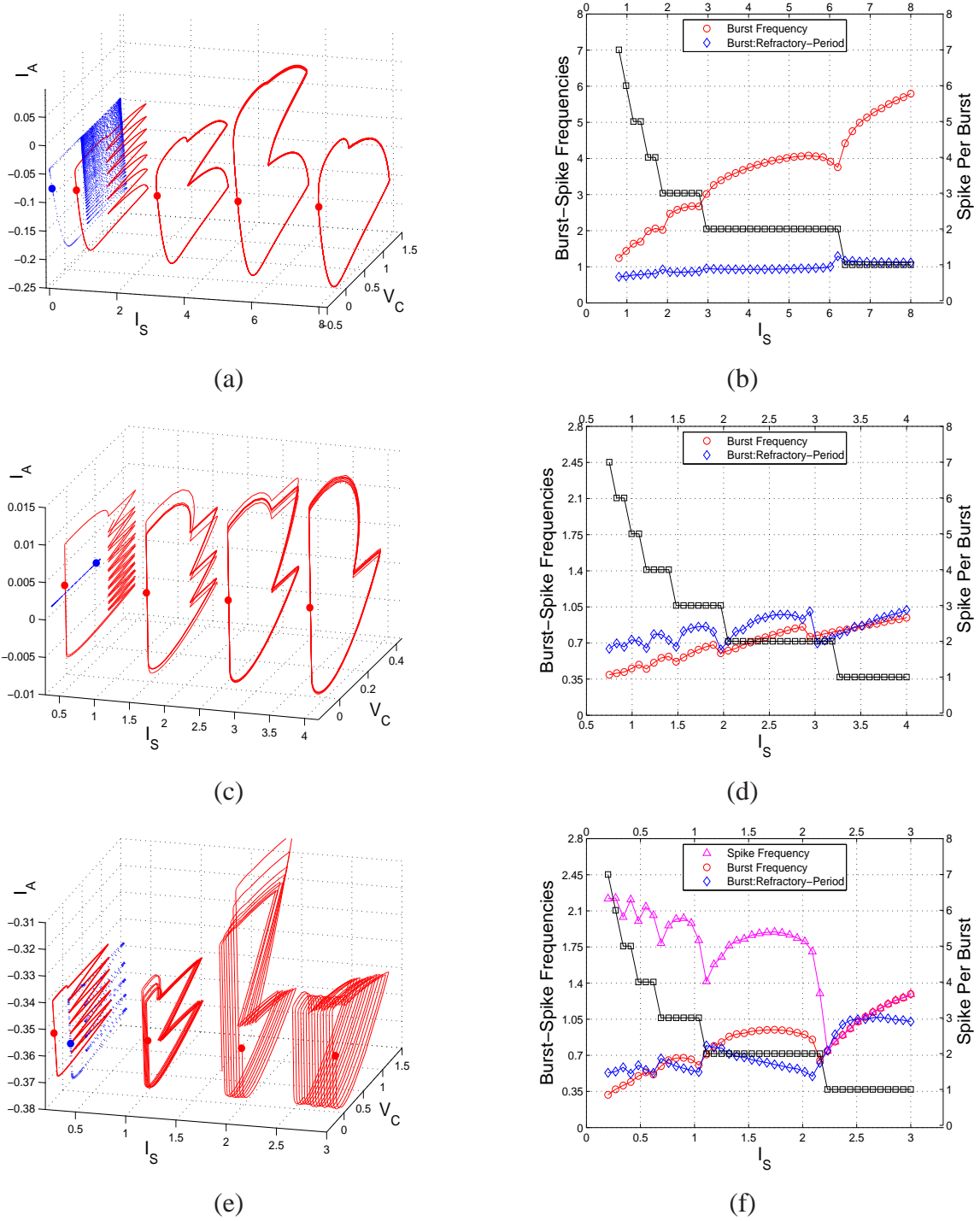


Figure 3: Metastability and plasticity simulations for various models. (a,b) pK⁺sNa⁺ model with the cubic IV -curves. Parameter values: $v_1 = 0.5$, $v_2 = 2.5$, $g_K + d_K = -1$, $i_1 = 0.25$, $i_2 = 0.8$, $\frac{1}{g_{Na}} + \frac{1}{d_{Na}} = -2.27$, $\bar{E}_{Na} = 0.6$, $\bar{E}_K = -0.7$, $C = 0.01$, $\lambda = 0.5$, $\gamma = 0.1$, $I_{ext} = 0$, $\epsilon = 0.0005$. (c,d) pNa⁺sK⁺ model with the piecewise-linear IV -curves. Parameter values: $g_{Na} = 1$, $d_{Na} = -1.21$, $v_1 = -0.7$, $v_2 = -0.2$, $\bar{E}_{Na} = 0.6$, $g_K = 0.17$, $d_K = -0.08$, $i_1 = 0.18$, $i_2 = 0.5$, $\bar{E}_K = -0.7$, $C = 0.01$, $\lambda = 0.05$, $\gamma = 0.1$, $I_{ext} = 0$, $\epsilon = 0.0005$. (e,f) pK⁺_{-d}sNa⁺_{+d} model with the same parameter values as Fig.2 except for $\gamma_{Na} = 0.1$, $\gamma_K = 0.05$, $\lambda_{Na} = 0.05$, $\lambda_K = 0.1$.

corresponding native spike-burst lies in the subspace $I_A = -I_S$. Again, for the same reason as above, metastable-plastic spike-bursts cannot exist without the additional dimension provided by the I_S -variable.

4. Discussions. The main result of this paper can be summarized as follows.

1. $pX_{\pm}yY_{\mp}$ and $pX_{\pm d}yY_{\mp d}$ models with $y = c$ and s can generate metastable-plastic action potentials of varying frequencies at different absolute ion pump currents.
2. $pX_{\pm}sY_{\mp}$ and $pX_{\pm d}sY_{\mp d}$ models can generate metastable-plastic spike-bursts of varying isospike numbers at different absolute ion pump currents.
3. The plastic spike-bursts of $pX_{\pm}sY_{\mp}$ and $pX_{\pm d}sY_{\mp d}$ models are arranged in the order of natural number progression in their isospike numbers against the absolute ion pump current.
4. The action potentials and spike-bursts of $pX_{\pm}yY_0$ models with $y = c$ and/or s cannot be plastic.

These results cannot be derived from Hodgkin-Huxley type models ([9, 6, 12, 11, 1, 10, 8, 3]) because the latter do not distinguish neurons' ion pump dynamics from their electro and diffusive counterparts.

Many open questions remain. For examples, what is the largest isospike number that a given neuron model can have? How is it related to the native spike-burst? If this largest isospike number is finite, what is the optimal range in the isospike numbers that a neuron model should have? How does a communication system work based on the assumption that the metastable-plastic spike-bursts are information alphabet? Last and perhaps most importantly, does the phenomenon of ion-pump-mediated metastability and plasticity exist in real neurons? These questions and conceivably many more need to be explored elsewhere. A few of which will be studied in [5].

Acknowledgement: Special thanks to Jack Hale and Shui-Nee Chow who believed in the project in its inception when the outcome was nothing but uncertain.

References

- [1] Chay, T.R. and J. Keizer, *Minimal model for membrane oscillations in the pancreatic beta-cell*, Biophys J., **42**(1983), pp.181-190.
- [2] Chua, L.O., *Introduction to Nonlinear Circuit Theory*, McGraw-Hill, New York, 1969.
- [3] Deng, B., *A mathematical model that mimics the bursting oscillations in pancreatic β -cells*, Math. Biosciences, **119**(1993), pp.241-250.

- [4] Deng, B., *General circuit models of neurons with ion pump*, preprint, (2007).
(<http://www.math.unl.edu/~bdeng1/Papers/DengNeuroCircuit.pdf>)
- [5] Deng, B., *Quadrature spike code for optimal neural communication and informational preference to Golden Ratio distribution*, preprint, (2007).
(<http://www.math.unl.edu/~bdeng1/Papers/DengNeuralCodePreferences.pdf>)
- [6] FitzHugh, R., *Impulses and physiological states in models of nerve membrane*, Biophys. J., **1**(1961), pp.445–466.
- [7] Hagiwara, S. and H. Morita, *Coding mechanisms of electroreceptor fibers in some electric fish*, J. Neurophysiol. **26**(1963), pp.551–567.
- [8] Hindmarsh, J.L. and R.M. Rose, *A model of neuronal bursting using three coupled first order differential equations*, Proc. R. Soc. Lond. B. **221**(1984), pp.87–102.
- [9] Hodgkin, A.L. and A.F. Huxley, *A quantitative description of membrane current and its application to conduction and excitation in nerve*, J. Physiol. **117**(1952), pp.500–544.
- [10] Keener, J.P., *Analog circuitry for the van der Pol and FitzHugh-Nagumo Equations*, IEEE Trans. on Systems, Man, and Cybernetics, **13**(1983), pp.1011–1015.
- [11] Morris, C. and H. Lecar, *Voltage oscillations in the barnacle giant muscle fiber*, Biophysical J., **35**(1981), pp.193–213.
- [12] Nagumo, J., S. Arimoto, and S. Yoshizawa, *An active pulse transmission line simulating nerve axon*, Proc. IRE, **59**(1964), pp.2061–2070.
- [13] Perkel, D.H., T.H. Bullock, *Neural coding*, Neurosci. Res. Prog. Sum. **3**(1968), pp.405–527.